Digestive Diseases and Sciences
https://doi.org/10.1007/s10620-025-09574-y

ORIGINAL ARTICLE

High *INHBB* Expression Shapes an Immunosuppressive Tumor Microenvironment and Predicts Poor Prognosis in Colorectal Carcinoma

Hiroshi Sawaguchi[1] · Takeshi Uehara[2] · Mai Iwaya[2] · Shiho Asaka[2,3] · Tomoyuki Nakajima[2] · Shotaro Komamura[2] · Shunsuke Imamura[1] · Yugo Iwaya[1] · Shinsuke Sugenoya[4] · Masato Kitazawa[4] · Yuji Soejima[4] · Hiroyoshi Ota[2,5] · Tadanobu Nagaya[1]

Received: 30 October 2025 / Accepted: 16 November 2025

Abstract

Background Inhibin subunit beta B (*INHBB*), a member of the TGF-β superfamily, has emerged as a potential regulator of tumor progression and immune modulation. However, its clinical and immunological significance in colorectal cancer (CRC) remains unclear.

Methods This study evaluated *INHBB* mRNA expression in 248 CRC cases using RNA in situ hybridization (RNAscope), immunohistochemistry (IHC), and single-cell RNA sequencing (scRNA-seq). Associations with clinicopathological parameters, tumor-infiltrating immune cells, and prognosis were analyzed.

Results *INHBB* was primarily expressed in tumor epithelial cells and weakly in stromal cells, but was negligible in normal mucosa. High *INHBB* expression correlated significantly with venous invasion, lymph node metastasis, advanced TNM stage, and reduced tumor-infiltrating lymphocytes. IHC revealed marked decreases in $CD4^+$, $CD8^+$, and $FOXP3^+$ T cells and increased $CD163^+$ tumor-associated macrophages in *INHBB* high tumors, indicating an immunosuppressive tumor microenvironment (TME). Kaplan–Meier analysis showed that high *INHBB* expression was associated with worse overall survival and recurrence-free survival, but was not an independent prognostic factor in multivariate models.

Conclusion *INHBB* is predominantly expressed in tumor epithelium and is associated with aggressive features, poor prognosis, and the formation of an immune-cold, macrophage-rich TME in CRC. These findings suggest that *INHBB* may be a potential biomarker for immune evasion and a target for novel immunotherapeutic strategies in CRC.

Keywords *INHBB* · Colorectal carcinoma · Tumor microenvironment

✉ Takeshi Uehara
tuehara@shinshu-u.ac.jp

[1] Division of Gastroenterology and Hepatology, Department of Medicine, Shinshu University School of Medicine, Matsumoto, Japan

[2] Department of Laboratory Medicine, Shinshu University School of Medicine, 3-1-1 Asahi, Matsumoto, Nagano 390-8621, Japan

[3] Department of Laboratory Medicine and Pathology, Life Science Research Center, Nagano Children's Hospital, Azumino, Japan

[4] Division of Gastroenterological, Hepato-Biliary-Pancreatic, Transplantation and Pediatric Surgery, Department of Surgery, Shinshu University School of Medicine, Matsumoto, Japan

[5] Department of Clinical Laboratory Sciences, Shinshu University School of Medicine, Matsumoto, Japan

Abbreviations

ARGs	Anoikis-related genes
CRC	Colorectal carcinoma
CAFs	Cancer-associated fibroblasts
CEA	Carcinoembryonic antigen
GEO	Gene Expression Omnibus
TCGA	The Cancer Genome Atlas
IRS	Immunoreactivity score
ISH	In situ hybridization
OS	Overall survival
RFS	Recurrence-free survival
scRNA-seq	Single-cell RNA sequencing
TIL	Tumor-infiltrating lymphocytes
TMA	Tissue microarray
TME	Tumor microenvironment

Published online: 01 December 2025

Introduction

Colorectal carcinoma (CRC) is one of the most common gastrointestinal malignancies, with more than 1.9 million new cases diagnosed annually worldwide. It ranks as the second leading cause of cancer-related mortality worldwide after lung cancer, and remains the second leading cause of cancer death in the United States [1]. Although CRC is potentially curable with early detection and appropriate treatment, advanced-stage cases are often associated with high rates of recurrence and metastasis, resulting in a poor prognosis. Specifically, the 5-year survival rate for early-stage disease (stage I) exceeds 90%, with recurrence rates kept below 10%. In contrast, advanced cases—particularly those with metastasis or stage III or higher—exhibit recurrence rates of 20–30%, and the 5-year survival is significantly reduced to approximately 15–20% [2–4]. Therefore, in addition to conventional staging systems such as TNM classification and serum markers like CEA, the identification of more accurate prognostic indicators and the establishment of personalized therapeutic strategies have become urgent clinical needs.

One biological process gaining attention in relation to cancer invasion and metastasis is anoikis, a form of programmed cell death induced by detachment from the extracellular matrix. The acquisition of resistance to anoikis by tumor cells is closely associated with increased malignancy and metastatic potential. Analyses targeting anoikis-related genes (ARGs) are thus expected to contribute to the discovery of novel prognostic biomarkers and therapeutic targets [5]. Among these, *inhibin subunit beta B* (*INHBB*), a member of the TGF-β superfamily, is a component of activin B and inhibin B, originally described in the context of endocrine regulation. More recently, *INHBB* has been implicated in a variety of tumor-associated processes, including cell proliferation, differentiation, apoptosis, fibrosis, and immune response modulation [6]. Elevated *INHBB* expression has been reported to correlate with malignant features and poor prognosis in various cancers, including hepatocellular carcinoma, clear cell renal cell carcinoma, and head and neck cancer [6–10]. Conversely, in nasopharyngeal carcinoma, *INHBB* may have tumor-suppressive effects related to promoting apoptosis and suppressing metastasis [11], suggesting that its role may be context-dependent across tumor types.

In CRC, several bioinformatics analyses using public datasets such as TCGA and GEO have suggested that high *INHBB* expression is associated with poor overall survival (OS), increased invasiveness and metastatic potential, and the development of an immunosuppressive TME. For example, Wu et al. identified *INHBB* as an anoikis-related gene in colon adenocarcinoma (COAD) and reported that its high expression correlated with worse prognosis, the activation of cancer-associated fibroblasts (CAFs), and enrichment of immune-related pathways [12]. Similarly, Jia et al. and Xin et al. demonstrated that multigene prognostic models including *INHBB* predicted high recurrence risk and the presence of immunosuppressive features in CRC patients [13, 14]. Furthermore, elevated *INHBB* expression was associated with the increased infiltration of regulatory T cells (Tregs) and Th17 cells, as well as co-expression with immune checkpoint molecules such as PD-1 and CTLA-4, suggesting its potential involvement in shaping the tumor immune microenvironment [6, 15]. Although these findings suggest a role for *INHBB* in modulating the immune cell composition, most of the current evidence is derived from bulk RNA-seq data or immunohistochemistry (IHC), which lack spatial resolution within tumor tissues.

RNA in situ hybridization (RNA-ISH) enables the sensitive and spatially resolved detection of mRNA expression in formalin-fixed tissue sections. Recent advances in RNAscope technology allow for the quantitative assessment of gene expression at the single-cell level within a histological context [16]. In this study, we evaluated the expression of *INHBB* mRNA in CRC using RNA-ISH, aiming to elucidate its clinical and pathological relevance from a spatial and histological perspective.

Materials and Methods

Patients

This study included 305 cases of CRC treated surgically at Shinshu University Hospital between 2014 and 2022. All patients were monitored for a minimum follow-up period of 2 years. Tumor differentiation was assessed, with well-differentiated, moderately-differentiated, and poorly-differentiated adenocarcinomas included in the analysis. Based on previously published criteria [17], well-differentiated and moderately-differentiated adenocarcinomas were classified as low-grade, whereas poorly-differentiated adenocarcinomas were categorized as high-grade. Among these patients, 57 cases were excluded for the following reasons: 40 cases were negative for the positive control (housekeeping gene) in the TMA, and 17 cases had no tumor tissue at the primary site within a TMA. Ultimately, 248 cases of CRC were enrolled.

Clinical and pathological data, including patient age, sex, tumor differentiation, prognosis, lymph node involvement, vascular invasion, tumor-infiltrating lymphocytes (TILs), and TNM classification, were extracted from medical records. Tumor staging and differentiation were defined following the eighth edition of the Union for International Cancer Control (UICC) classification [18] and the fifth

edition of the World Health Organization (WHO) classification [19]. Histological evaluation of all specimens was independently performed by two pathologists (T.U. and M.I.). TILs in tumor-infiltrating regions were scored using a four-tier system: 0 (none), 1 (mild), 2 (moderate), and 3 (marked) [20]. For subsequent analyses, TIL scores were categorized as low (scores 0 and 1) or high (scores 2 and 3).

OS was defined as the duration between the date of surgical resection and death or last follow-up. Recurrence-free survival (RFS) was defined as the time from surgical resection to disease recurrence or the last follow-up without recurrence. This study adhered to the ethical principles outlined in the Declaration of Helsinki and received approval from the Clinical Trial Review Committee of Shinshu University School of Medicine (approval number: 5836).

Histopathology and Tissue Microarray (TMA) Construction

All specimens were fixed in 10 or 20% neutral-buffered formalin and embedded in paraffin. For the construction of a TMA, blocks containing sufficient tumor tissue from the invasive frontline were selected from formalin-fixed paraffin-embedded tissue archives. Tissue cores (3-mm diameter) were punched out from each block using thin-walled stainless steel needles (Azumaya Medical Instruments Inc., Tokyo, Japan) and arrayed into a recipient paraffin block. Serial 4-μm-thick sections were cut from the TMA blocks, and one section was stained with hematoxylin and eosin for histological assessment.

Immunohistochemistry and Evaluation

IHC staining for CD4, CD8, FOXP3, and CD163 was performed on serial TMA sections to evaluate immune cell subsets. The staining was carried out using a fully automated staining system (BOND-III; Leica Biosystems, Newcastle, UK) with the following primary antibodies: CD4 (clone 4B12, ready-to-use; Leica Biosystems), CD8 (clone C8/144B, ready-to-use; Leica Biosystems), FOXP3 (clone 236A/E7, 1:100 dilution; Abcam, UK), and CD163 (clone 10D6, ready-to-use; Leica Biosystems).

The evaluation methods differed by marker. For $CD4^+$, $CD8^+$, and $FOXP3^+$ T cells, three areas with the highest cell density were selected from each core, and cell counts per high-power field (HPF; 10 × ocular, 40 × objective) were performed. An average of the three fields was used for analysis, and the median of these counts served as the cutoff to classify cases into low and high infiltration groups. For CD163, expression was evaluated semiquantitatively using the immunoreactivity score (IRS), which was calculated by multiplying the staining intensity (SI; 0–3 scale) by the percentage of positive cells (PP; 0–4 scale), as previously described [21]. Cases were then classified into high and low CD163 expression groups based on the median IRS value.

All histological features and staining results were independently evaluated by two experienced pathologists (T.U. and M.I.).

INHBB RNA In Situ Hybridization

The detection of *INHBB* mRNA was performed using the RNAscope® LS 2.5 Probe – Hs-*INHBB* (cat. no. 435748; Advanced Cell Diagnostics, Hayward, CA, USA) according to the manufacturer's instructions, using unstained sample tissue slides. Briefly, tissue sections were pretreated with heat and protease prior to hybridization as previously described [22]. Brown punctate dots observed in the nucleus or cytoplasm were considered positive signals. Standard Mm-PPIB (ACD-313902) was used as a positive control to ensure interpretable results.

INHBB expression was quantified under a 40 × objective lens (Olympus BX53 microscope) according to the five-grade scoring system recommended by the manufacturer: no staining (0), 1–3 dots/cell (1 +), 4–9 dots/cell (2 +), 10–15 dots/cell and/or < 10% dots in clusters (3 +), and > 15 dots/cell and/or > 10% dots in clusters (4 +). For further analysis, samples were classified into low *INHBB* expression (grades 0, 1 +, and 2 +) and high *INHBB* expression (grades 3 + and 4 +). We analyzed the association between *INHBB* expression and clinicopathological parameters and prognosis in patients with CRC.

Single-Cell RNA Sequencing Analysis of *INHBB* Expression in CRC

The single-cell RNA sequencing (scRNA-seq) analysis of *INHBB* expression was conducted using a publicly available dataset (Accession Number: GSE132465) obtained from the NCBI Gene Expression Omnibus (GEO) database. This dataset comprised 23 tumor samples and 10 normal samples derived from CRC tissues. Data processing and analysis were conducted using the Seurat R package (v4.1.0). Raw count matrices were normalized to a total expression of 10,000 molecules per cell and subsequently scaled. Highly variable genes across cells were identified and utilized for principal component analysis (PCA) to reduce dimensionality. To assess cellular similarities and perform clustering, the FindNeighbors and FindClusters functions were used. The visualization of cellular heterogeneity was achieved by applying uniform manifold approximation and projection (UMAP) using the RunUMAP function. The expression distribution of *INHBB* marker genes was assessed across the clusters, allowing for cell type annotation.

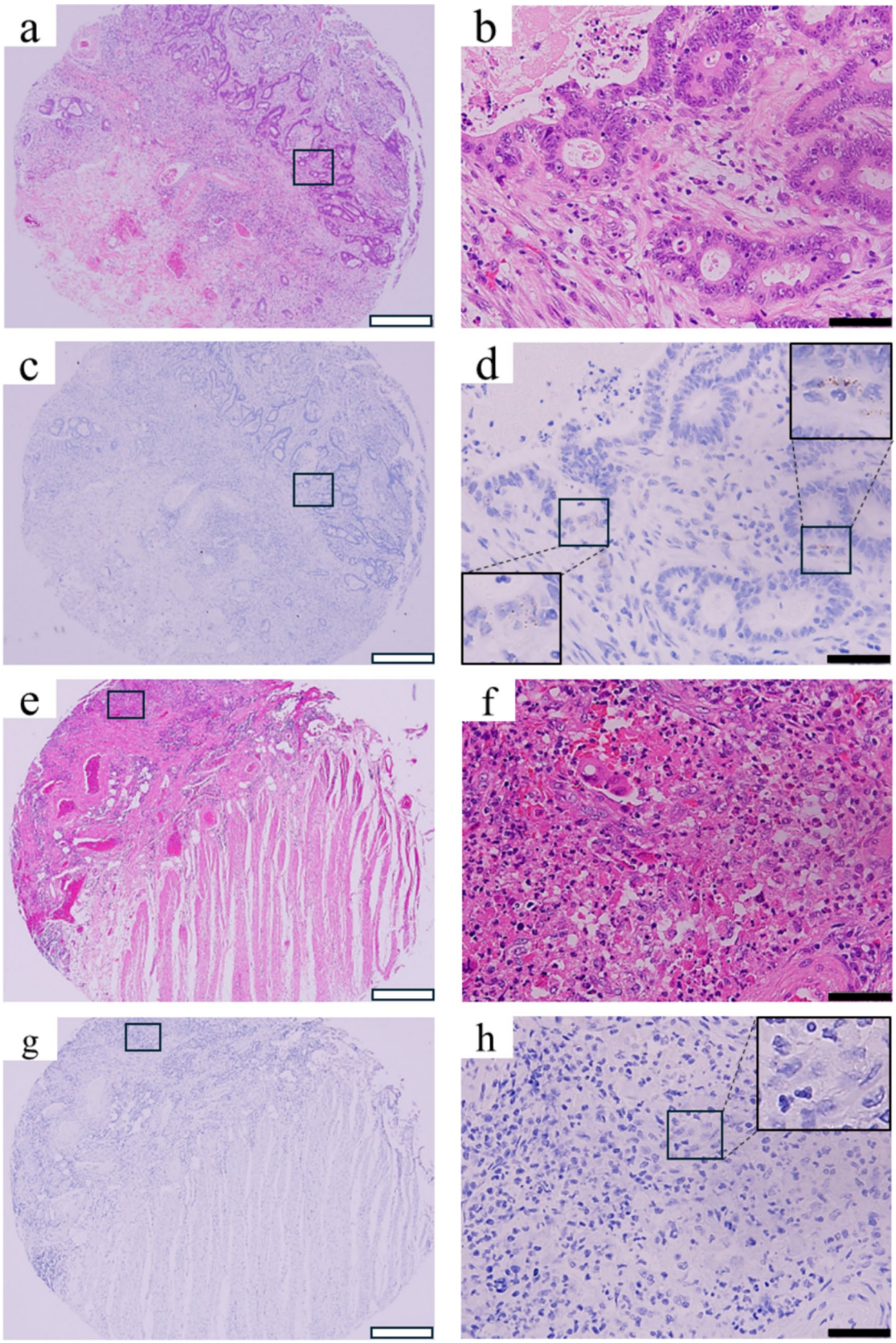
a
b
c
d
e
f
g
h

◂**Fig. 1** RNA in situ hybridization (RNA-ISH) and H&E staining for *INHBB* expression in colorectal carcinoma. Representative hematoxylin and eosin (H&E) staining images in cases with high (**a**, **b**) and low (**e**, **f**) *INHBB* expression. Corresponding RNA-ISH images in high-expression (**c**, **d**) and low-expression (**g**, **h**) cases are also shown. Low-power (**a**, **c**, **e**, **g**) and high-power (**b**, **d**, **f**, **h**) images are displayed. In high-expression cases, brown punctate *INHBB* mRNA signals were observed in tumor epithelial and stromal areas (**d**). In contrast, such signals were barely detectable in low-expression cases (**h**). Black scale bars = 50 µm; white scale bars = 500 µm

Statistical Analysis

Categorical variables were expressed as frequencies, and differences between subgroups were assessed using Fisher's exact test. The Mann–Whitney *U*-test was used to compare immune cell infiltration levels ($CD4^+$, $CD8^+$, $CD163^+$, and $FOXP3^+$ cells) between the *INHBB* high-expression and low-expression groups. To visualize the distribution of immune cell counts, violin plots were generated using the ggplot2 package. The OS was analyzed in the entire cohort of 248 patients (stage 0–IV) and the RFS analysis was limited to 202 patients with non-metastatic (stage 0–III) disease. The OS and RFS were estimated by the Kaplan–Meier method, and between-group comparisons were performed using the log-rank test. Prognostic factors were analyzed through univariate and multivariate Cox proportional hazards regression models. Statistical significance was defined as $p < 0.05$. All statistical analyses were performed using EZR (Easy R), version 1.66, a graphical interface for R developed by the R, Foundation for Statistical Computing (Vienna, Austria).

Results

Association Between *INHBB* Expression and the Clinicopathological Features of CRC

INHBB-positive signals appeared as brown punctate dots in tumor epithelial cells and the tumor stroma (Fig. 1a–d). Representative histological images of *INHBB*-negative cases are shown in Fig. 1e–h. Notably, *INHBB* expression was not observed in histologically normal colorectal mucosa. Among the 248 CRC cases included in the tissue microarray (TMA), 210 had detectable *INHBB* expression. Based on the scoring criteria, 88 cases were classified as high *INHBB* expression ($\geq 3+$ score).

The relationship between *INHBB* expression and clinicopathological parameters is summarized in Table 1. There were no significant differences in age, sex, or tumor differentiation between the high and low expression groups. However, high *INHBB* expression was significantly associated with venous invasion ($p = 0.005$), tumor-infiltrating lymphocyte (TIL) score ($p = 0.003$), $CD4^+$ T cells ($p = 0.002$), $CD8^+$ T cells ($p = 0.032$), and $CD163^+$ cells ($p = 0.038$). The infiltration levels of $CD4^+$, $CD8^+$, and $FOXP3^+$ T cells tended to be lower in the high *INHBB* expression group, indicating a negative association. In contrast, $CD163^+$ cell levels were significantly higher in tumors with high *INHBB* expression, suggesting a positive association. Although $FOXP3^+$ T cells showed a decreasing trend in the high-expression group, the difference did not reach statistical significance ($p = 0.063$). Additionally, high *INHBB* expression was strongly correlated with lymph node metastasis ($p < 0.001$) and advanced pathological stage (Stage III–IV, $p < 0.001$).

Correlation Between *INHBB* Expression and Tumor-Infiltrating Immune Cells

To explore the immunological features associated with *INHBB* expression further, tumors were stratified into low and high expression groups, and the infiltration of $CD4^+$, $CD8^+$, $FOXP3^+$ T cells, and $CD163^+$ cells was assessed by immunohistochemistry. Violin plots of immune cell counts in each group are presented in Fig. 2.

Mann–Whitney *U*-test analysis revealed that the numbers of $CD4^+$ ($p = 0.005$), $CD8^+$ ($p < 0.001$), and $FOXP3^+$ ($p = 0.028$) T cells were significantly lower in the high *INHBB* expression group compared with the low expression group. Conversely, $CD163^+$ cells were significantly increased in tumors with high *INHBB* expression ($p = 0.008$). Representative immunostaining patterns in tumors with low and high *INHBB* expression are shown in Figs. 3 and 4, respectively.

Prognostic Impact of *INHBB* Expression on the Overall Survival

Kaplan–Meier analysis demonstrated that high *INHBB* expression was significantly associated with shorter OS compared with low *INHBB* expression (log-rank $p = 0.004$; Fig. 5). Univariate Cox proportional hazards analysis identified tumor differentiation (HR 2.25, 95% CI 1.02–4.98, $p = 0.045$), TIL score (HR 0.24, 95% CI 0.11–0.52, $p < 0.001$), $FOXP3^+$ T cells (HR 0.25, 95% CI 0.12–0.51, $p < 0.001$), lymph node metastasis (HR 3.27, 95% CI 1.64–6.53, $p < 0.001$), advanced pathological stage (HR 3.85, 95% CI 1.84–8.08, $p < 0.001$), and high *INHBB* expression (HR 2.42, 95% CI 1.31–4.48, $p = 0.005$) as significant prognostic factors for OS (Table 2).

Multivariate analysis demonstrated that lymphatic invasion (HR 2.27, 95% CI 1.03–4.97, $p = 0.041$) and advanced stage (HR 2.63, 95% CI 1.17–5.95, $p = 0.02$) remained independent prognostic factors, whereas *INHBB* expression did not retain statistical significance as an independent predictor (HR 1.64, 95% CI 0.85–3.18, $p = 0.142$).

Table 1 *INHBB* expression and clinicopathological characteristics of patients with colorectal carcinoma

Factors	$n=248$	*INHBB* expression		
		Low ($n=160$)	High ($n=88$)	p value
Age				0.69
< 70 years	112	74	38	
≥ 70 years	136	86	50	
Sex				0.501
Male	146	97	49	
Female	102	63	39	
Histological grade				0.186
Low	213	141	72	
High	35	19	16	
Lymphatic invasion				0.085
Present	122	72	50	
Absent	126	88	38	
Venous invasion				**0.005**
Present	179	106	73	
Absent	69	54	15	
TIL				**0.003**
High	122	90	32	
Low	126	70	56	
CD4				**0.002**
High	115	87	28	
Low	128	72	56	
CD8				**0.032**
High	125	89	36	
Low	120	69	51	
FOXP3				0.063
High	124	87	37	
Low	121	71	50	
CD163				**0.038**
High	101	59	42	
Low	138	99	39	
LN metastasis				***p* < 0.001**
Present	115	51	64	
Absent	133	109	24	
TNM stage				***p* < 0.001**
0–II	127	107	20	
III–IV	121	53	68	

LN lymph node

Bold indicate statistical significance at p 0.05

Prognostic Impact of *INHBB* Expression on Recurrence-Free Survival

Similarly, Kaplan–Meier analysis revealed that patients with high *INHBB* expression had significantly worse RFS compared with those with low *INHBB* expression (log-rank $p=0.024$; Fig. 5).

In univariate analysis, lymphatic invasion (HR 3.05, 95% CI 1.32–7.07, $p=0.009$), advanced TNM stage (HR 4.65, 95% CI 1.94–11.14, $p<0.001$), and high *INHBB* expression (HR 2.40, 95% CI 1.10–5.28, $p=0.029$) were significant prognostic factors for RFS (Table 3). In multivariate analysis, only TNM stage remained an independent prognostic factor for RFS (HR 4.65, 95% CI 1.94–11.14, $p<0.001$), and high *INHBB* expression did not reach statistical significance (HR 1.43, 95% CI 0.62–3.32, $p=0.405$).

Spatial and Single-Cell Expression Analysis of *INHBB* Using scRNA-seq

To investigate the cellular origin of *INHBB* expression, we performed scRNA-seq analysis using publicly available CRC datasets. UMAP dimensionality reduction was used to visualize cellular clusters in tumor and normal tissues (Fig. 6). In tumor tissues, distinct clusters of epithelial cells, T cells, B cells, mast cells, myeloid cells, and stromal cells were identified (Fig. 6a). Similar clusters were also observed in normal tissues (Fig. 6b).

INHBB expression was predominantly localized to the epithelial cell clusters in tumor tissues, with weak expression also detected in subsets of stromal cells (Fig. 6c). In contrast, *INHBB* expression in normal tissues was minimal overall, with negligible expression in epithelial cells and scattered low-level expression in stromal cells (Fig. 6d).

Discussion

In this study, we comprehensively investigated the significance of *INHBB* expression in CRC using RNA-ISH, immunohistochemistry, and scRNA-seq. Our findings demonstrated that high *INHBB* expression was significantly associated with aggressive tumor characteristics, including advanced stage and lymph node metastasis, as well as the decreased infiltration of T cells, increased tumor-associated macrophages (TAMs), and shorter OS and RFS.

The key novel finding of this study is the spatial and cellular characterization of *INHBB* expression using RNA-ISH and scRNA-seq. Although *INHBB* mRNA was virtually undetectable in normal colonic epithelium, it was predominantly expressed in tumor epithelial cells. This suggests that tumor cells themselves may actively produce and secrete *INHBB*, potentially contributing to the establishment of an immunosuppressive TME through autocrine and/or paracrine signaling. Furthermore, weak *INHBB* expression was also observed in a subset of stromal cells, likely including CAFs, supporting the notion that epithelial–stromal

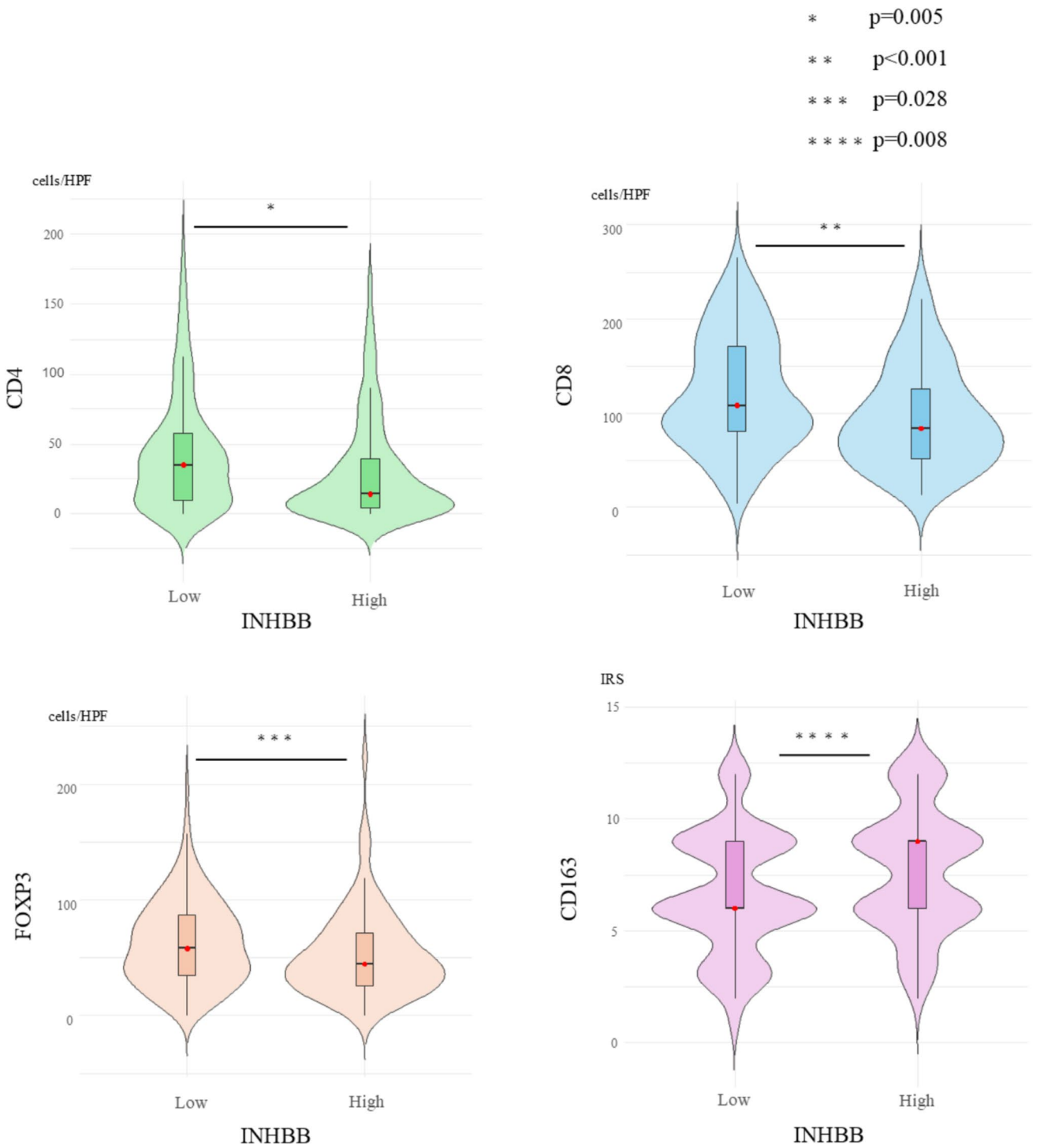

Fig. 2 Association between *INHBB* expression and tumor-infiltrating immune cells. Violin plots showing the distribution of $CD4^+$, $CD8^+$, and $FOXP3^+$ T cells, and $CD163^+$ cells according to *INHBB* expression levels. A Mann–Whitney *U*-test indicated the significantly lower infiltration of $CD4^+$ ($p=0.005$), $CD8^+$ ($p<0.001$), and $FOXP3^+$ ($p=0.028$) T cells in the high *INHBB* expression group. In contrast, $CD163^+$ cells were significantly increased in the high-expression group ($p=0.008$)

interactions may collaboratively promote immune evasion via *INHBB*, in agreement with the findings of Wu et al. [12].

IHC analysis revealed a significantly reduced intratumoral infiltration of $CD4^+$ and $CD8^+$ T cells in tumors with high *INHBB* expression. Notably, $FOXP3^+$

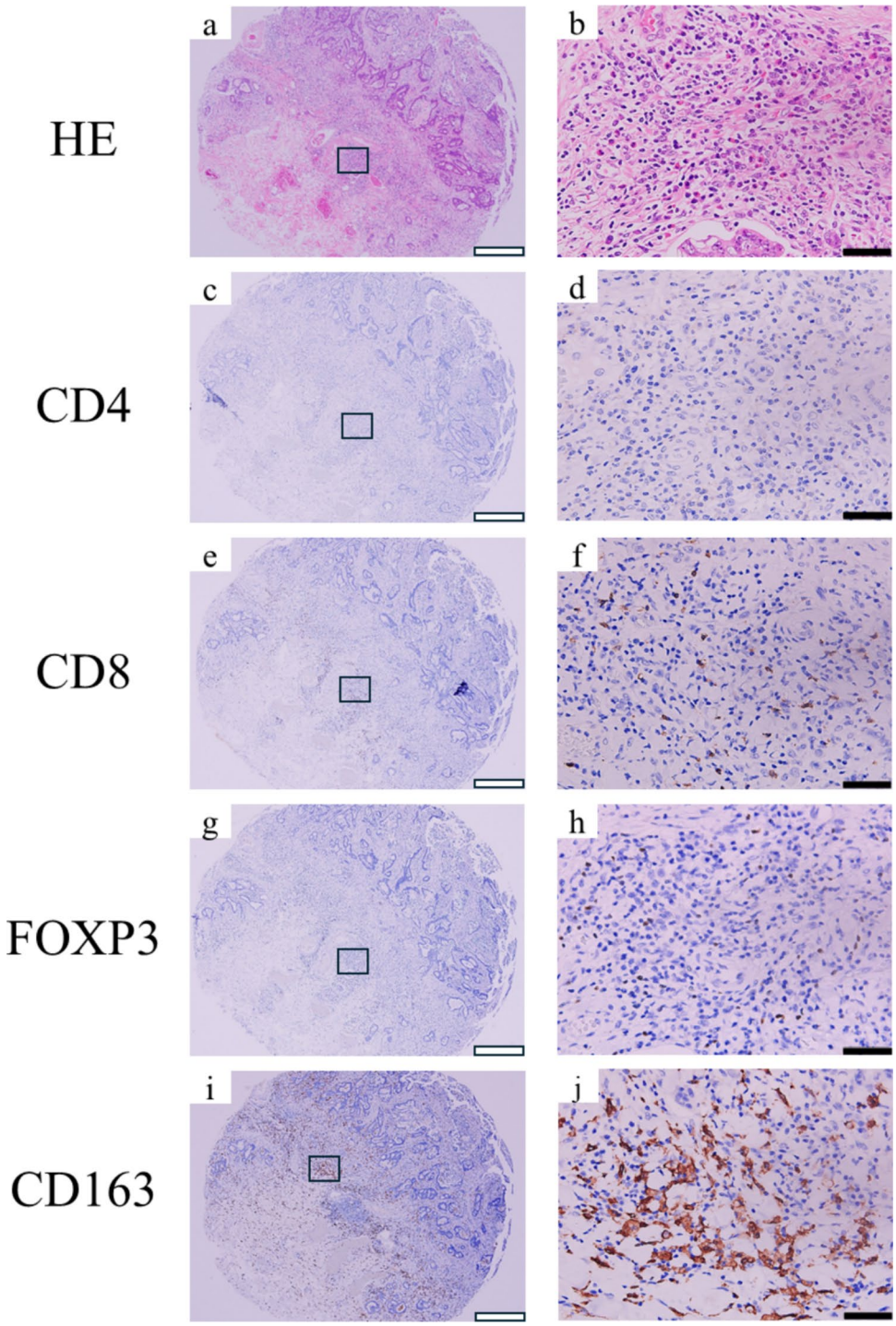

Fig. 3 Immunohistochemical staining of CD4, CD8, FOXP3, and CD163 in a case with high *INHBB* expression. Representative H&E staining near TILs in a high *INHBB* expression case (**a**, **b**). Immunostaining for $CD4^+$ (**c**, **d**), $CD8^+$ (**e**, **f**), and $FOXP3^+$ (**g**, **h**) T cells showed only sparse infiltration at low and high magnification. In contrast, $CD163^+$ cells (**i**, **j**) were abundantly present on the TMA. Black scale bars = 50 µm; white scale bars = 500 µm

regulatory T cells also showed a significant decrease in cell number ($p = 0.028$) when directly quantified. These T cell subsets play central roles in antitumor immune responses, and their diminished infiltration is indicative of an "immune-cold" or "immune-desert" TME [23–25]. In particular, the reduction of $CD8^+$ cytotoxic T cells may reflect impaired cell-mediated immunity and might contribute to resistance against immune checkpoint blockade therapy.

Of particular interest, $CD163^+$ TAMs—a hallmark of immunosuppressive M2 macrophages—were significantly more abundant in the high *INHBB* expression group. CD163 is a marker for M2-type TAMs, which produce anti-inflammatory cytokines, suppress T cell activation, and promote angiogenesis, all of which support tumor

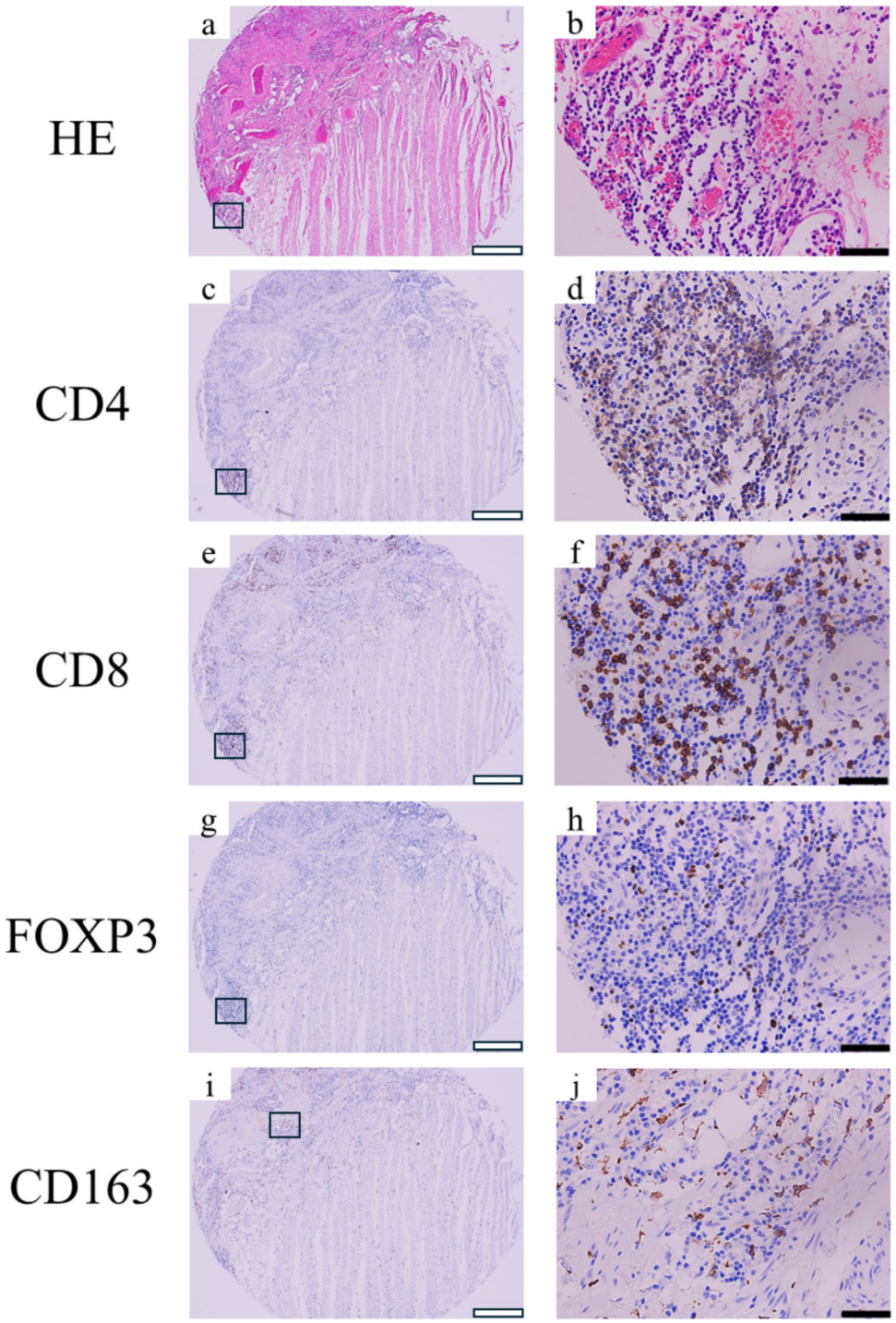

Fig. 4 Immunohistochemical staining of CD4, CD8, FOXP3, and CD163 in a case with low *INHBB* expression. Representative H&E staining near TILs in a low *INHBB* expression case (**a**, **b**). $CD4^+$ (**c**, **d**), $CD8^+$ (**e**, **f**), and $FOXP3^+$ (**g**, **h**) T cells were strongly stained positive. In contrast, $CD163^+$ cells (**i**, **j**) were weakly expressed on the TMA. Black scale bars = 50 μm; white scale bars = 500 μm

immune evasion [13, 26, 27]. These results suggest that high *INHBB* expression may suppress T cell infiltration and induce M2 macrophage polarization, thereby remodeling the TME into a broadly immunosuppressive state.

As a member of the TGF-β superfamily, *INHB*B functions as a subunit of activin B and is implicated in fibrosis and immune regulation. Recent studies have shown that activin B promotes M2 macrophage differentiation and activates

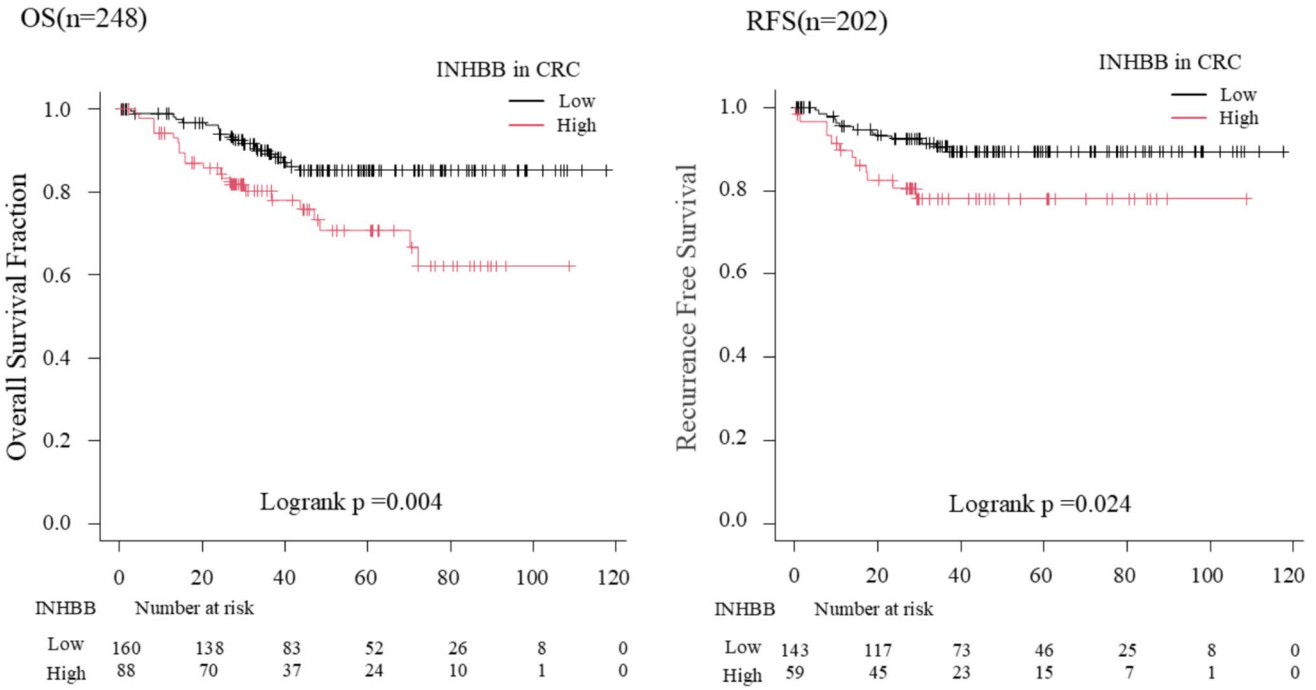

Fig. 5 Kaplan–Meier survival analysis stratified by *INHBB* expression. Patients were stratified into two groups based on *INHBB* expression levels, and OS and RFS were evaluated by Kaplan–Meier analysis. The left panel shows OS ($n=248$, log-rank $p=0.004$) and the right panel shows RFS ($n=202$, log-rank $p=0.024$). High *INHBB* expression was significantly associated with poorer prognosis in both analyses

Table 2 Univariate and multivariate analyses of overall survival factors in CRC

Factors	Univariate analysis				Multivariate analysis				
	HR	95%CI		*p*-value	HR	95%CI			*p*-value
Age ≥ 70 years vs. < 70 years	0.90	0.49	– 1.66	0.74	0.95	0.5	–	1.8	0.882
Sex: male vs. female	1.16	0.63	– 2.15	0.634	1.14	0.61	–	2.1	0.681
Histological grade: low vs. high	2.25	1.02	– 4.98	**0.045**					
Lymphatic invasion: absent vs. present	3.52	1.72	– 7.17	***p* < 0.001**	2.27	1.03	–	4.97	**0.041**
Venous invasion: absent vs. present	1.96	0.87	– 4.41	0.106					
TIL low vs. high	0.24	0.11	– 0.52	***p* < 0.001**					
CD4 low vs. high	0.71	0.38	– 1.32	0.277					
CD8 low vs. high	0.62	0.33	– 1.16	0.137					
FOXP3 low vs. high	0.25	0.12	– 0.51	***p* < 0.001**					
CD163 low vs. high	0.80	0.42	– 1.56	0.517					
LN metastasis: absent vs. present	3.27	1.64	– 6.53	***p* < 0.001**					
TNM stage: 0-II vs. III–IV	3.85	1.84	– 8.08	***p* < 0.001**	2.63	1.17	–	5.95	**0.02**
INHBB expression: low vs. high	2.42	1.31	– 4.48	**0.005**	1.64	0.85	–	3.18	0.142

LN lymph node

Bold indicate statistical significance at *p* 0.05

Table 3 Univariate and multivariate analyses of recurrence-free survival factors in CRC

Factors	Univariate analysis					Multivariate analysis				
	HR	95%CI			*P*-value	HR	95%CI			*P*-value
Age ≥ 70 years vs. < 70 years	1.33	0.59	–	3.01	0.493					
Sex: male vs. female	1.17	0.53	–	2.57	0.700					
Histological grade: low vs. high	1.46	0.50	–	4.28	0.488					
Lymphatic invasion: absent vs. present	3.05	1.32	–	7.07	**0.009**	1.71	0.68	–	4.34	0.256
Venous invasion: absent vs. present	1.63	0.65	–	4.09	0.294					
TIL low vs. high	0.85	0.39	–	1.86	0.681					
CD4 low vs. high	1.28	0.58	–	2.82	0.538					
CD8 low vs. high	1.06	0.48	–	2.32	0.895					
FOXP3 low vs. high	1.11	0.50	–	2.47	0.798					
CD163 low vs. high	1.24	0.57	–	2.73	0.586					
TNM stage: 0-II vs. III	4.65	1.94	–	11.14	***p* < 0.001**	4.65	1.94	–	11.14	***p* < 0.001**
INHBB expression: low vs. high	2.40	1.10	–	5.28	**0.029**	1.43	0.62	–	3.32	0.405

LN lymph node

Bold indicate statistical significance at p 0.05

CAFs, thereby exacerbating the immunosuppressive remodeling of the TME [15, 28]. The increased infiltration of $CD163^+$ cells observed in our study aligns with these prior reports.

Moreover, previous bioinformatic analyses have identified correlations between high *INHBB* expression and reduced T cell infiltration, CAFs activation, and the elevated expression of immune checkpoint molecules such as PD-1 and CTLA-4 [12, 29, 30]. Our findings of reduced T cell presence and increased TAMs in *INHBB*-high tumors are consistent with these reports. Importantly, our study extends these insights by providing spatially and cell type-resolved evidence through RNA-ISH and scRNA-seq, offering mechanistic support to existing transcriptomic data.

Prognostically, *INHBB* high expression was significantly associated with shorter OS and RFS. Although *INHBB* did not emerge as an independent prognostic factor in multivariate analysis, the observed reduction in T cell infiltration and increase in M2 TAMs suggest that *INHBB* contributes to tumor progression and immune evasion, which may ultimately lead to poor clinical outcomes.

Collectively, our findings indicate that *INHBB* likely promotes tumor progression in CRC by simultaneously suppressing antitumor immune responses and fostering an immunosuppressive TME. These findings highlight the potential of *INHBB* as a therapeutic target and predictive biomarker in CRC.

Nonetheless, several limitations of this study warrant consideration. First, the use of TMA may not fully capture intratumoral spatial heterogeneity, especially with respect to TIL distribution and immune cell localization. Second, the observational nature of the study precludes the direct inference of causality between *INHBB* expression and immune modulation. Functional validation studies, such as knockdown or overexpression assays and co-culture experiments, as well as in vivo modeling, are needed to confirm the mechanistic role of *INHBB*. Third, we did not directly assess the expression of immune checkpoint molecules (e.g., PD-1, CTLA-4); therefore, comparisons with previous studies are based on inferred immune cell patterns rather than direct molecular evidence.

Conclusions

Our study suggests that *INHBB* promotes an immunosuppressive tumor microenvironment in CRC by reducing T cell infiltration and increasing M2-type macrophage recruitment. These immune alterations are associated with tumor progression and poor prognosis. Future studies should elucidate the immunoregulatory mechanisms of *INHBB* further and evaluate its potential as a therapeutic target. In particular, *INHBB* may be a predictive biomarker or combinatorial target in immunotherapeutic strategies, including immune checkpoint blockade and macrophage-targeted therapies.

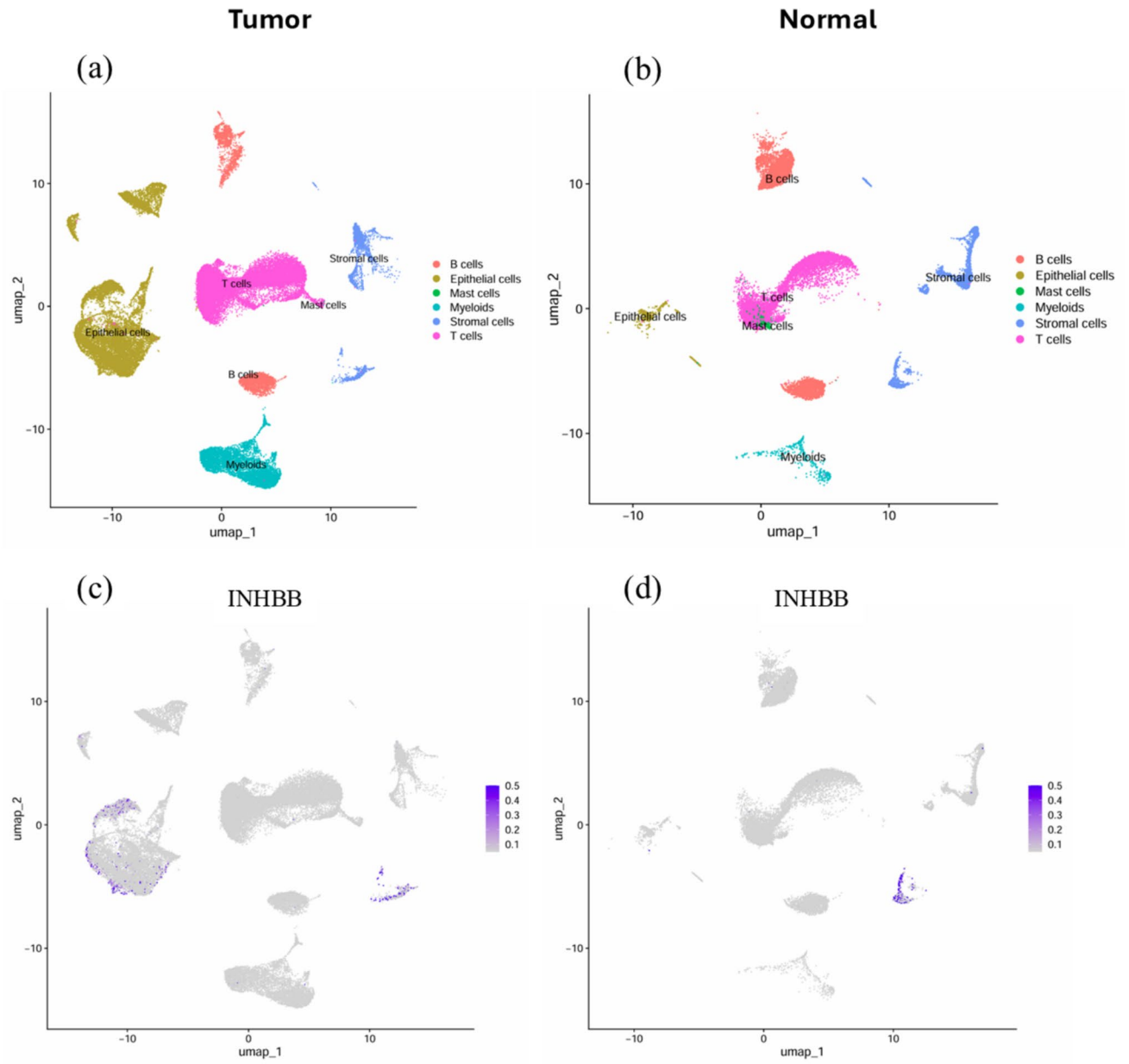

Fig. 6 Spatial distribution of *INHBB* expression based on single-cell RNA sequencing (scRNA-seq). **a**, **b** UMAP plots visualizing cell clusters in tumor (**a**) and normal (**b**) tissues. Identified clusters included epithelial cells, T cells, B cells, mast cells, myeloid cells, and stromal cells. **c**, **d** Distribution of *INHBB* expression. In tumor tissues (**c**), *INHBB* was primarily expressed in epithelial cells, with weak expression also seen in some stromal cell clusters. In normal tissues (**d**), *INHBB* expression was negligible in epithelial cells and was detected sporadically in stromal cells

Acknowledgments We thank Masanobu Momose, Yasuyo Shimojo, Chitose Arai, Kanade Wakabayashi, Naoko Yamaoka, Saki Mukai, Daiki Ogura, Daiki Gomyo, and Tsukane Seki at Shinshu University Hospital for their excellent technical assistance. We also thank Kelly Zammit, BVSc, and J. Ludovic Croxford, PhD, from Edanz (https://jp.edanz.com/ac) for editing a draft of this manuscript.

Author Contributions Hiroshi Sawaguchi participated in the design of the study, performed the pathological analysis, and drafted the manuscript. Takeshi Uehara and Mai Iwaya helped perform the pathological analysis. Takeshi Uehara performed the statistical analysis. Hiroshi Sawaguchi, Tomoyuki Nakajima, and Shotaro Komamura performed the TMA construction and RNAscope analysis. Shinsuke Sugenoya, Yugo Iwaya, and Masato Kitazawa examined the clinical data. Takeshi Uehara, Mai Iwaya, Shiho Asaka, Hiroyoshi Ota, Yuji Soejima, and Tadanobu Nagaya critically revised the draft manuscript. All authors have read and approved the manuscript.

Funding This research received no specific grant from any funding agency in the public, commercial, or not-for-profit sectors.

Data availability All data generated and analyzed during the current study are available from the corresponding author on reasonable request.

Declarations

Competing interests The authors declare no competing interests.

Consent for publication Not applicable.

Clinical trial number Not applicable.

Ethical approval and consent to participate The ethics committee of Shinshu University School of Medicine approved this study (Approval Code: 5836) and waived the requirement for informed consent. An opt-out method was used because of the retrospective design of the study. The investigation was conducted in compliance with the Declaration of Helsinki.

References

1. Siegel RL, Giaquinto AN, Jemal A. Cancer statistics, 2024 *CA Cancer J Clin*. 2024;74:12–49.
2. Nors J, Iversen LH, Erichsen R, Gotschalck KA, Andersen CL. *Incidence of Recurrence and Time to Recurrence in Stage I to III Colorectal Cancer: A Nationwide Danish Cohort Study JAMA Oncol.* 2024;10:54–62.
3. Osterman E, Glimelius B. Recurrence Risk After Up-to-Date Colon Cancer Staging, Surgery, and Pathology: Analysis of the Entire Swedish Population. *Dis Colon Rectum*. 2018;61:1016–1025.
4. Gately L, Jalali A, Semira C et al. *Stage dependent recurrence patterns and post-recurrence outcomes in non-metastatic colon cancer Acta Oncol.* 2021;60:1106–1113.
5. Guo T, Wang Y. *Expression of Anoikis-Related Genes and Potential Biomarkers in Colon Cancer Based on RNA-seq and scRNA-seq Appl Biochem Biotechnol.* 2024;196:8282–8305.
6. Liu Y, Zhou Q, Zou G, Zhang W. Inhibin subunit beta B (INHBB): an emerging role in tumor progression *J Physiol Biochem*. 2024;80:775–793.
7. Chung YY, Cheng SJ, Ko HH, Shie WY, Elizabeth Chou HY. *Evaluation of the prognostic and therapeutic potential of inhibin beta B for oral squamous cell carcinoma J Dent Sci.* 2024;19:448–454.
8. Chen Y, Qian B, Sun Xet al. . Sox9/INHBB axis-mediated crosstalk between the hepatoma and hepatic stellate cells promotes the metastasis of hepatocellular carcinoma *Cancer Lett*. 2021;499:243–254.
9. Wacker I, Behrens J. *Activin B antagonizes RhoA signaling to stimulate mesenchymal morphology and invasiveness of clear cell renal cell carcinomas PLoS One.* 2014;9:e111276.
10. Yang X, Jia Q, Zou Z et al. *INHBB promotes tumor aggressiveness and stemness of glioblastoma via activating EGFR signaling Pathol Res Pract.* 2023;245:154460.
11. Zou G, Ren B, Liu Y et al. *Inhibin B suppresses anoikis resistance and migration through the transforming growth factor-beta signaling pathway in nasopharyngeal carcinoma Cancer Sci.* 2018;109:3416–3427.
12. Wu Q, Ye L, Wu Y et al. *Combining single-cell analysis and molecular docking techniques to construct a prognostic model for colon adenocarcinoma and uncovering inhibin subunit betab as a novel therapeutic target Front Immunol.* 2024;15:1524560.
13. Jia X, Zhang T, Lv X, Du H, Sun Y, Guan Y. *Identification of the six-hormone secretion-related gene signature as a prognostic biomarker for colon adenocarcinoma Cancer Biomark*. 2023;38:523–535.
14. Xin C, Lai Y, Ji Let al. . A novel 9-gene signature for the prediction of postoperative recurrence in stage II/III colorectal cancer *Front Genet*. 2022;13:1097234.
15. Yuan J, Xie A, Cao Q, Li X, Chen J. *INHBB Is a Novel Prognostic Biomarker Associated with Cancer-Promoting Pathways in Colorectal Cancer Biomed Res Int.* 2020;2020:6909672.
16. Wang F, Flanagan J, Su Net al. . RNAscope: a novel in situ RNA analysis platform for formalin-fixed, paraffin-embedded tissues *J Mol Diagn*. 2012;14:22–29.
17. Fleming M, Ravula S, Tatishchev SF, Wang HL. *Colorectal carcinoma: Pathologic aspects J Gastrointest Oncol.* 2012;3:153–173.
18. Brierley JD GM, Wittekind C. TNM classification of malignant tumours. John Wiley & Sons. 2017.
19. Nagtegaal ID AM OR, Lam AK. Tumours of the colon and rectum. In: Board WCoTE, ed.^eds. *WHO Classification of Tumours: Digestive System Tumours*, City; International Agency for Research on Cancer (IARC);2020.
20. Ropponen KM, Eskelinen MJ, Lipponen PK, Alhava E, Kosma VM. Prognostic value of tumour-infiltrating lymphocytes (TILs) in colorectal cancer *J Pathol*. 1997;182:318–324.
21. Wei C, Yang C, Wang S et al. *Crosstalk between cancer cells and tumor associated macrophages is required for mesenchymal circulating tumor cell-mediated colorectal cancer metastasis Mol Cancer.* 2019;18:64.
22. Ukpo OC, Flanagan JJ, Ma XJ, Luo Y, Thorstad WL, Lewis JS, Jr. High-risk human papillomavirus E6/E7 mRNA detection by a novel in situ hybridization assay strongly correlates with p16 expression and patient outcomes in oropharyngeal squamous cell carcinoma *Am J Surg Pathol*. 2011;35:1343–1350.
23. Liu JL, Yang M, Bai JG, Liu Z, Wang XS. "Cold" colorectal cancer faces a bottleneck in immunotherapy *World J Gastrointest Oncol*. 2023;15:240–250.
24. Wu B, Zhang B, Li B, Wu H, Jiang M. *Cold and hot tumors: from molecular mechanisms to targeted therapy Signal Transduct Target Ther.* 2024;9:274.
25. Zheng S, Wang W, Shen L, Yao Y, Xia W, Ni C. Tumor battlefield within inflamed, excluded or desert immune phenotypes: the mechanisms and strategies *Exp Hematol Oncol*. 2024;13:80.
26. Xue T, Yan K, Cai Yet al. . Prognostic significance of CD163+ tumor-associated macrophages in colorectal cancer *World J Surg Oncol*. 2021;19:186.
27. Chen Y, Song Y, Du W, Gong L, Chang H, Zou Z. *Tumor-associated macrophages: an accomplice in solid tumor progression J Biomed Sci.* 2019;26:78.
28. Yu W, He G, Zhang W, Ye Z, Zhong Z, Huang S. *INHBB is a novel prognostic biomarker and correlated with immune infiltrates in gastric cancer Front Genet.* 2022;13:933862.
29. Yin Y, Yang S, Huang Z, Yang Z, Zhang C, He Y. *RNA methylation-related genes INHBB and SOWAHA are associated with MSI status in colorectal cancer patients and may serve as prognostic*

markers for predicting immunotherapy efficacy Carcinogenesis. 2024;45:337–350.
30. Zhao X, Li X, Miao Z. *Identification and validation of regulatory T cell-associated gene signatures to predict colon adenocarcinoma prognosis Int Immunopharmacol.* 2024;132:112034.